PCCP

PAPER

View Article Online
View Journal | View Issue

Cite this: *Phys. Chem. Chem. Phys.*, 2015, **17**, 14115

The influence of source molecule structure on the low temperature growth of nitrogen-doped graphene†

Tokio Katoh,[a] Gaku Imamura,[bc] Seiji Obata,[b] M. Bhanuchandra,[d] Graeme Copley,[d] Hideki Yorimitsu[de] and Koichiro Saiki*[ab]

Received 8th April 2015,
Accepted 1st May 2015

DOI: 10.1039/c5cp02032h

www.rsc.org/pccp

Doping of heteroatoms such as nitrogen into the lattice structure of graphene can tune and tailor the overall electronic properties. N-doped graphene, depending on the nitrogen bonding mode and/or bonding configuration, displays subtly altered properties in comparison to pristine graphene. However, there remains a disappointing shortage of reliable methods for introducing dopants in a controlled and reproducible manner, preventing a thorough understanding of the relationship between structure and properties. In this study we aimed to prepare graphenes with nitrogen atoms doped at a graphitic (quaternary) site by depositing a source molecule containing a graphitic nitrogen atom: 4,4,8,8,12,12-hexamethyl-8,12-dihydro-4*H*-benzo[9,1]quinolizino[3,4,5,6,7-*defg*]acridine or 4*H*-benzo[9,1]quinolizino[3,4,5,6,7-*defg*]acridine-4,8,12-trione, on a heated Pt(111) substrate. At 400 °C, graphene with nitrogen atoms exclusively doped at a graphitic site was synthesized from the former molecule, while not from the latter molecule at any temperature. The present result indicates that the rational design of a source molecule is quite important for controlling the nitrogen doped site in the graphene lattice.

1. Introduction

Graphene is a single layer of graphite which consists of sp^2 carbon atoms bonded in a hexagonal lattice. Since its first isolation in 2004,[1] graphene has attracted much attention due to its extraordinary properties such as high carrier mobility,[2] high thermal conductivity,[3] high surface area,[4,5] and high Young's modulus.[6] The electronic properties of graphene could be modified by doping heteroatoms like boron[7–9] or nitrogen.[10–16] For example, theoretical and experimental studies have proved that B or N doping provides a band gap in graphene[10,17,18] and the energy gap can be tuned by the concentration and the site of doped atoms.[18,19] Especially nitrogen-doped graphene has attracted much attention due to its potential use in technological applications such as fuel cells,[20,21] lithium ion batteries,[22–24] and ultracapacitors.[25] Although various kinds of studies have been reported focusing on the synthesis of nitrogen doped graphene, control of the doped sites and understanding of its effects on the electronic properties have not been fully established.

Nitrogen doping is usually achieved in two ways: direct synthesis and post treatment.[26] Chemical vapor deposition (CVD) is a promising direct synthesis method for preparing a large-area and high-quality nitrogen doped graphene.[27,28] We had previously conducted CVD growth of pristine and nitrogen doped graphenes on Pt(111).[29–33] Platinum is chemically stable and less contaminated compared to copper or other transition metals on which graphene can be grown. Pt does not need hydrogen during the CVD growth of graphene, making it possible to synthesize nitrogen doped graphene from a single source molecule. This is favorable for the discussion on the growth mechanism of nitrogen doped graphene by pursuing the relationship between the properties of the product and the source molecule species. Another advantage of using a Pt substrate is its rather weak interaction with graphene[30] and thus the properties of the grown graphene are less affected by the substrate. In addition, graphene could be transferred from Pt onto SiO_2 by a bubbling transfer method.[34]

In our previous work, we have examined the growth of nitrogen doped graphene on Pt(111) from source molecules such as pyridine (C_5H_5N), acrylonitrile (C_3H_3N), and hexaphenylborazine

[a] *Department of Chemistry, School of Science, The University of Tokyo, Kashiwanoha 5-1-5, Kashiwa, Chiba 277-8561, Japan*
[b] *Department of Complexity Science and Engineering, Graduate School of Frontier Sciences, The University of Tokyo, Kashiwanoha 5-1-5, Kashiwa, Chiba 277-8561, Japan. E-mail: saiki@k.u-tokyo.ac.jp; Fax: +81-4-7136-3903; Tel: +81-4-7136-5526*
[c] *World Premier International (WPI) Research Center, International Center for Materials Nanoarchitectonics (MANA), National Institute for Materials Science (NIMS), 1-1 Namiki, Tsukuba, Ibaraki 305-0044, Japan*
[d] *Department of Chemistry, Graduate School of Science, Kyoto University, Sakyo-ku, Kyoto 606-8502, Japan*
[e] *ACT-C, JST, Sakyo-ku, Kyoto 606-8502, Japan*

† Electronic supplementary information (ESI) available. See DOI: 10.1039/c5cp02032h

($B_3N_3H_6$, HPB).[31,32] Except acrylonitrile, nitrogen doped graphene was formed by depositing the source molecules on a heated Pt substrate only at the temperatures equal to or lower than 500 °C. The nitrogen atoms are doped mostly at a pyridinic site in the pyridine-derived graphene and at a pyridinic site in the BN grains in the HPB-derived graphene. Nitrogen atoms are likely to be incorporated at the periphery of the graphene grains not within the graphene lattice. Since the doped site affects the electronic structure of graphene,[35] a method to control the doped site is urgently required.

Here we report the growth of nitrogen doped graphene from new molecular sources. We have selected a source molecule in which a nitrogen atom is surrounded by carbon atoms in a graphitic form. We are interested mainly in doping nitrogen inside the lattice not at the periphery. We deposited the molecule on the heated Pt(111) surface, and the product was characterized by low energy electron diffraction (LEED), X-ray photoelectron spectroscopy (XPS), and Raman spectroscopy.

2. Experimental section

2.1. Source molecules

As a source molecule, we chose two compounds: 4,4,8,8,12,12-hexamethyl-8,12-dihydro-4*H*-benzo[9,1]quinolizino[3,4,5,6,7-*defg*]-acridine (Fig. 1a) and 4*H*-benzo[9,1]quinolizino[3,4,5,6,7-*defg*]-acridine-4,8,12-trione (Fig. 1b). There is a subtle difference in their peripheral structure that bridges the benzene rings. For simplicity, the molecule that has three dimethylmethylene bridges is called the methyl-form and the other triketone molecule is referred to as the ketone-form. These compounds were prepared by following existing protocols.[36,37] In these molecules, each nitrogen atom is surrounded by three carbon atoms *via* a single bond and is tightly embedded in a graphitic manner in the molecular framework. We have confirmed the flatness of these molecules by DFT calculations as described in the ESI.† The structure of these molecules seems favorable for the incorporation of nitrogen atoms into the graphitic site of the graphene lattice during the CVD process.

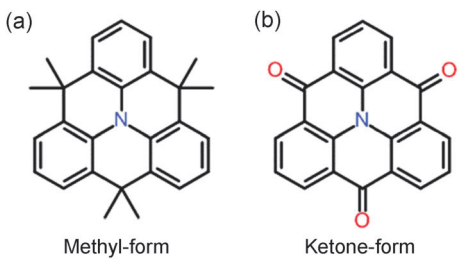

Fig. 1 Source molecules.

2.2. Film growth and characterization

Film growth by CVD and the surface analysis were conducted in an ultrahigh vacuum (UHV) chamber with the base pressure lower than 10^{-7} Pa. The Pt(111) substrate was mechanically polished and washed under sonication with acetone in open air. After being loaded into the UHV chamber, the substrate was cleaned by Ar ion sputtering and annealing. The substrate temperature (T_s) was determined using an infrared pyrometer at high temperatures and a thermocouple at lower temperatures. Before the CVD growth, the cleanness of the Pt(111) surface was confirmed by XPS. Both molecules were evaporated using a Knudsen cell in the UHV chamber. The deposition rate was 0.16 Å s^{-1} which was monitored using a quartz crystal microbalance (QCM). The film growth was continued until the total flux on Pt amounted to 30 nm by QCM. The as-grown film was transferred to the analysis chamber without breaking vacuum and characterized using XPS and LEED. XPS was carried out using Mg Kα radiation (1253.6 eV) (Thermo VG Scientific XR3E2) as an X-ray source and photoelectrons were analyzed using a hemispherical analyzer (SPECS, PHOIBOS-100, 5 channeltrons). To detect small peaks, the energy scan was repeated 480 times as the largest. The LEED analysis was performed using a MCP LEED apparatus (OCI BDL800IR) with a beam energy of 100 eV. After the XPS and LEED measurements in UHV, the film was transferred to a SiO_2 substrate by a bubbling method[34] for Raman measurements. The Raman spectrum was obtained using a JASCO NRS-3100 with a laser wavelength of 532 nm in atmosphere.

3. Results

3.1. Growth from methyl-form

The film derived from the methyl-form was characterized by LEED *in situ*. The film deposited at RT showed no structure

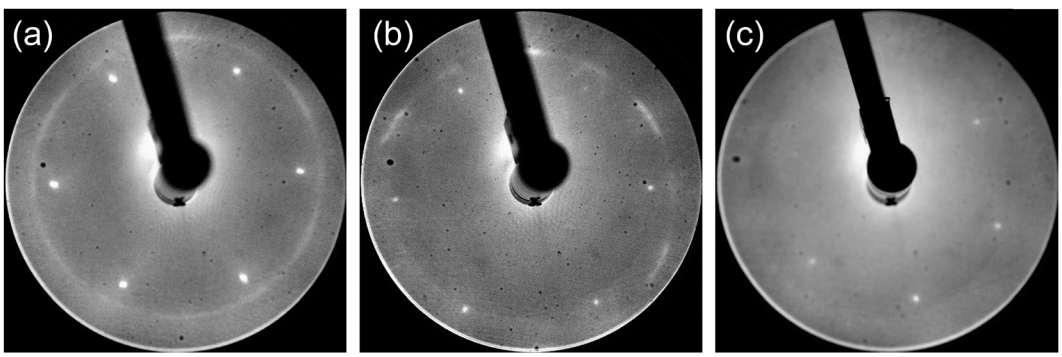

Fig. 2 LEED patterns of the methyl-form film deposited on Pt(111) at 300 °C (a), 400 °C (b), and 500 °C (c). The beam energy was 100 eV.

other than the six-fold spots of the Pt(111) substrate. Fig. 2 shows the LEED patterns of the film fabricated on Pt(111) at different T_s values: (a) 300 °C, (b) 400 °C, and (c) 500 °C. The six-fold sharp spots of the Pt(111) substrate were observed regardless of T_s. For the film grown at 300 °C, a faint ring structure was observed outside the six LEED spots of the Pt(111) surface as shown in Fig. 2a. Judging from the diameter of the ring, this diffraction pattern is ascribed to graphene with a high degree of rotational disorder. When the T_s was increased to 400 °C, the ring pattern changed into the arc-shape pattern as shown in Fig. 2b. The centers of the arcs are rotated by 30° with respect to the first order Pt spots. The arcs with 30° rotation were observed also for the graphene grown on Pt(111) at high temperatures.[38] When the T_s was further increased to 500–600 °C, the arcs disappeared and only the Pt-derived spots were observed as shown in Fig. 2c.

The deposited film was characterized by XPS to study the atomic concentration and the chemical state. Fig. 3a shows the wide-scan XPS spectra of Pt(111) before and after the deposition of methyl-form molecules at 400 °C. Several peaks can be observed which can be ascribed to Pt-derived lines. After depositing the methyl-form molecules, the C 1s peak appeared at around the binding energy of 284 eV. Fig. 3b shows the intensity ratio of C 1s (I_C) to Pt 4f (I_{Pt}) as a function of T_s. The amount of deposited carbon atoms decreases with increasing T_s. We have already found that monolayer graphene on Pt(111), which was grown from ethylene molecules, showed the intensity ratio of 0.034.[32] Therefore the amount of C atoms in the film deposited at 400 °C corresponds to that of a monolayer graphene.

High energy resolution spectra in the energy region of N 1s electrons are shown in Fig. 3c. The film deposited at RT has a peak centered at 400.0 eV. The nitrogen concentration is estimated to be 3.2 atomic percent (at%), which is close to the value of 3.7 at% in a methyl-form molecule within an accuracy of atom sensitivity factors. The film deposited at 300 °C has the binding energy and the nitrogen content almost similar to those at RT. For the film deposited at 400 °C, the N 1s peak was observed at 401.0 eV, and the concentration decreased to 2.0 at%. For the film deposited at T_s higher than 500 °C, no trace of N was discerned. Fig. 3d shows the nitrogen concentration as a function of T_s.

Fig. 4 shows the Raman spectra of the films deposited at various T_s values. The film deposited at RT could not be transferred to SiO_2, meaning reactions that produce large polymers did not occur. The spectrum at 300 °C shows broad and blurry peaks at around 1350 and 1600 cm^{-1}, which are assigned to the D and G band characteristics of carbon-based materials. There is no evidence of the formation of an sp^2 network and the spectrum is much more like amorphous carbon films rather than graphene. In the spectrum at 400 °C, on the other hand, the D and G bands were sharpened and a sharp 2D band appeared at around 2700 cm^{-1}, indicating the formation of a large network of sp^2 carbon atoms. Also, the peak appeared at around 3000 cm^{-1}, which is associated with the D + D′ peak.[39] The spectrum of 500 °C again showed broad D and G bands together with the disappearance of the 2D band.

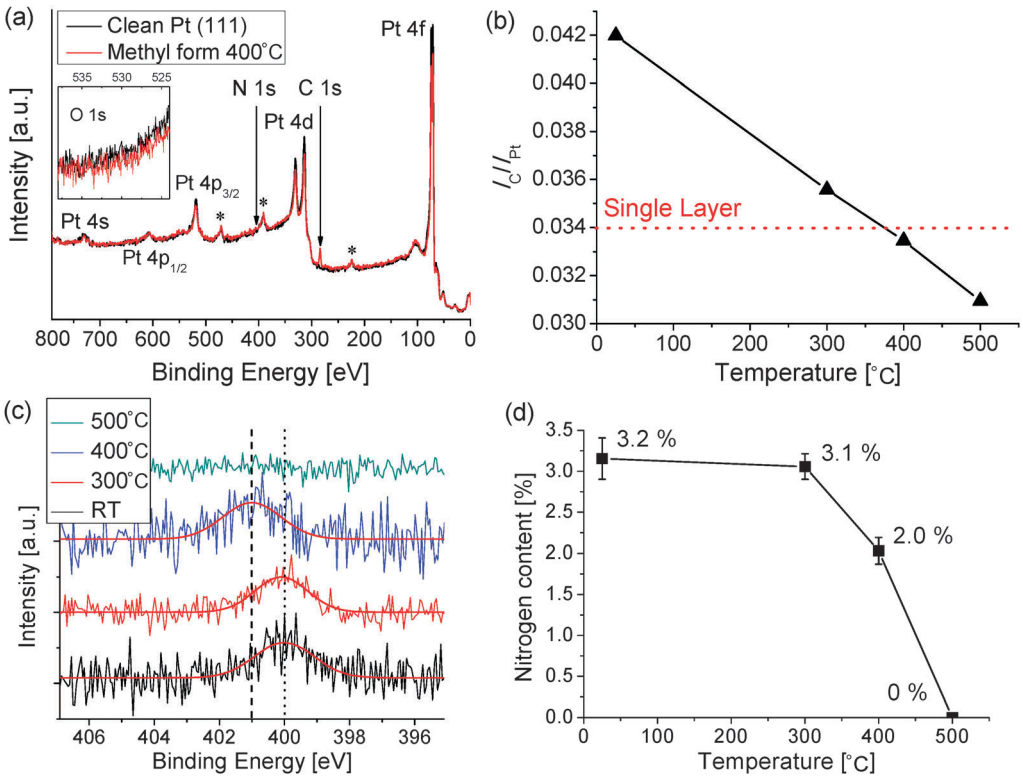

Fig. 3 (a) Wide range XPS spectra. *Peaks of Ta used as a substrate holder. (b) T_s dependence of C coverage. (c) High energy resolution XPS spectra in the N 1s region. (d) T_s dependence of nitrogen concentration.

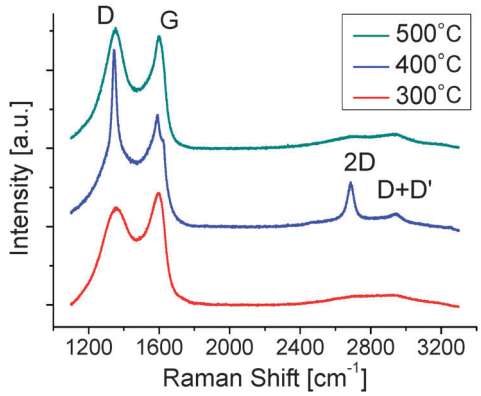

Fig. 4 Raman spectra of the methyl-form film deposited on Pt(111) at various T_s values and transferred onto the SiO_2 substrate.

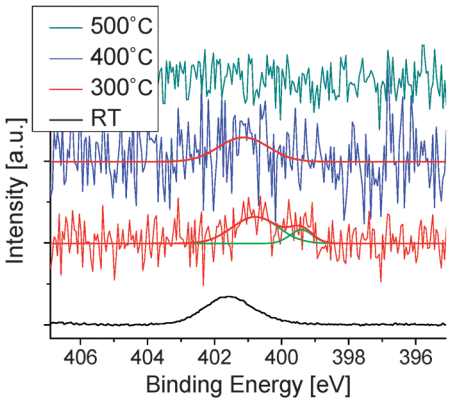

Fig. 6 High energy resolution XPS spectra in the N 1s region of ketone-form films.

From the Raman spectra, we found that the graphene lattice was formed only at a T_s of 400 °C.

3.2. Growth from ketone-form

To explore the effect of the difference in peripheral structure on the extent of graphenization and nitrogen doping, the ketone-form compound was also deposited on the Pt(111) surface at various T_s values. Fig. 5 shows the Raman spectra of the deposited films after being transferred onto SiO_2. The broad G and D bands are observed for the films at 300 °C and 400 °C. For the film deposited at 500 °C, the G and D bands become sharp and the 2D and D + D′ bands appear. Fig. 6 shows the high energy resolution XPS spectra in the region of N 1s electrons for the films deposited at various T_s values. A single peak centered at 401.7 eV was observed for the film fabricated at RT. The nitrogen content was 4.1 at%, which is close to that of the ketone-form molecule (4.7 at%). At a T_s of 300 °C, the nitrogen content decreased to 1.0 at% and the N 1s peak shifted to a lower binding energy side and split into two components. Simultaneously, the C 1s peak split into two components at RT and changed into a single component at 300 °C and the O 1s peak completely disappeared (Fig. S3, ESI†). These results indicate that the molecule was decomposed above a T_s of 300 °C. At 400 °C, a weak single peak was observed at a concentration of 0.4 at%. For T_s higher than 500 °C, no trace of nitrogen was observed within the S/N ratio of the XPS spectrum.

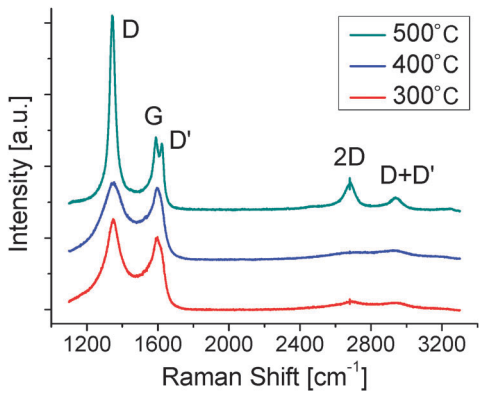

Fig. 5 Raman spectra of ketone-form films deposited at different T_s values and transferred onto the SiO_2 substrate.

4. Discussion

On the basis of characterization by LEED, XPS and Raman spectroscopy, we discuss the growth mechanism of nitrogen doped graphene from the methyl-form and ketone-form molecules. At first, we consider the film derived from the methyl-form molecule. At a T_s of 300 °C, the LEED pattern (Fig. 2a) shows an outer ring, indicating the formation of graphene-like grains oriented randomly with respect to one another.[38,40,41] The Raman spectrum in Fig. 4, however, corresponds to an amorphous-like carbon film. Diffraction patterns originating from the periodicity of atomic arrangement would appear for the nano-scale grains even if they are partially formed in the film. The absence of a graphene-like G-band in the Raman spectrum, on the other hand, suggests that π-conjugated electronic structure was not formed in the film deposited at 300 °C.

From these results, we propose the structure model as shown in Fig. 7a. The formation of a solid film transferrable to another substrate suggests that some of the methyl groups in the source molecules had been removed and that the triangle cores were instead bound with each other between the originally dimethylated carbon atoms. Several studies have reported such reactions where aromatic precursors coalesce with each other as a consequence of intermolecular C–C coupling.[42–44] The remaining part of the molecules would remain intact with the chemical state of the central nitrogen atom being unchanged, resulting in no chemical shift in the N 1s peak. The region in which the triangle cores are bound in the plane would give rise to the diffraction corresponding to the graphene-like periodicity but no G-band was observed in the π-conjugated structure. The part of triangle cores is not parallel to the surface owing to the partially remaining methyl groups.

When the T_s was increased to 400 °C, the G and 2D bands characteristic to the graphene lattice appeared, indicating the formation of π-conjugated electronic structures. At this stage,

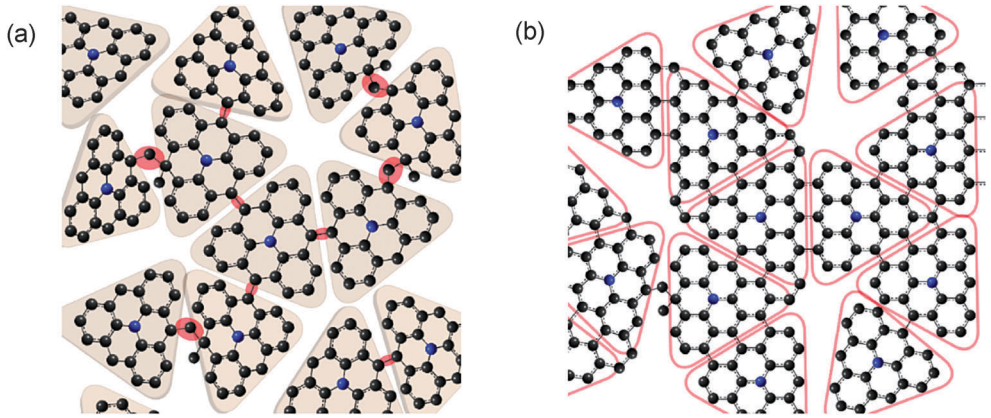

Fig. 7 Schematic illustration of possible structure formed from the methyl-form molecule at different T_s values: (a) 300 °C and (b) 400 °C, respectively. (a) The core structure of the molecule bonded with each other by a single bond. Part of triangle cores is out of the plane. (b) The core structure in the π-conjugated network with nitrogen at a quaternary site.

the source molecules would be more tightly fused *via* a similar reaction to dehydrogenation and C–C bond formation (Fig. 7b) as reported in several studies.[42–46] A large hump between G and D peaks in the Raman spectrum indicates the existence of a considerable amount of amorphous carbon region, and the large D intensity together with the appearance of D′ indicates many defects and the small grain size.[47,48] The shift in the binding energy of the N 1s peak to 401.0 eV also indicates such a fusion, since the quaternary N has a binding energy of 401.0 eV.[10,17,22,26,35] The selective appearance of graphitic nitrogen, which has been scarcely observed previously,[26] is a distinct characteristic of the nitrogen-doped graphene originating from the methyl-form molecule.

When T_s was increased further to 500 °C, the Raman spectrum again indicates the amorphous carbon film. The degree of graphenization decreased with increasing T_s, which is in sharp contrast to the CVD growth of graphene from small molecules such as methane.[49,50] If the decomposition of molecules generates carbon species to form graphene, the higher temperature would enhance graphenization.[31] The present model, however, does not mean the complete decomposition but the partial decomposition such as the removal of methyl groups. At T_s higher than 500 °C, decomposition is considered to proceed to the extent that the molecule could not retain its planeness.[44,45] Nevertheless the remaining carbon fragments decomposed at 500 °C are not so small as those that decomposed from methane at higher temperature. It seems difficult for such large fragments to form graphene *via* significant reorganization at 500 °C. The absence of nitrogen would come from the fact that the nitrogen containing fragments rapidly evaporate due to their higher volatility.[31] The discussion above also supports the growth model depicted in Fig. 7 in a sense that the methyl-form molecules partially decompose and are bound with each other.

The behavior of the ketone-form is very different from that of the methyl-form. Ketone-form could not form nitrogen doped graphene at any temperature. Oxygen disappeared even at 300 °C (Fig. S3, ESI†), which indicates the decomposition of the molecules. Transition metal surfaces including Pt are well known to facilitate the decarbonylation of carbonyl compounds.[51–54] We thus suppose that oxygen is desorbed as carbon monoxide to lose the original highly rigid structure. Although we have no exact ideas about chemical species formed at 300 °C, we assume the formation of more flexible species bearing no or less peripheral carbonyl linkers. The flexible species would be much easier to decompose further with loss of nitrogen. This loss of nitrogen would lead to the formation of the graphene lattice with a smaller content of nitrogen. The ketone-form molecule is almost completely decomposed at 500 °C and produces benzene or its fragments, leading to the formation of graphene without nitrogen.

5. Conclusions

N-doped graphene with nitrogen atoms exclusively at a graphitic site was synthesized by depositing the methyl-form molecules onto a Pt surface at 400 °C. The methyl-form molecules are bound without conjugation by removing the methyl groups at 300 °C, while the conjugation occurred locally at 400 °C leading to N-doped graphene. At 500 °C, an amorphous carbon film was grown due to the production of fragments inappropriate for graphenization. The ketone-form molecule did not form N-doped graphene at any temperature, while graphene growth occurred at 500 °C due to the production of benzene or its fragment. The interaction with a Pt surface seems to remove C–O from the ketone-form molecules at a temperature as low as 300 °C. Thus the peripheral substituents of the precursor molecules significantly affect the formation of N-doped graphene. We expect that the present result is beneficial for efficient structural design of a source molecule to achieve graphene with nitrogen atoms doped at a desired site.

Acknowledgements

This work was partially supported by a Grant-in-Aid for Scientific Research from MEXT of Japan (No. 25107002). The DFT calculations were performed at Research Center for Computational Science, Okazaki, Japan.

Notes and references

1 K. S. Novoselov, A. K. Geim, S. V. Morozov, D. Jiang, Y. Zhang, S. V. Dubonos, I. V. Grigorieva and A. A. Firsov, *Science*, 2004, **306**, 666–669.
2 K. I. Bolotin, K. J. Sikes, Z. Jiang, M. Klima, G. Fudenberg, J. Hone, P. Kim and H. L. Stormer, *Solid State Commun.*, 2008, **146**, 351–355.
3 A. A. Balandin, S. Ghosh, W. Bao, I. Calizo, D. Teweldebrhan, F. Miao and C. N. Lau, *Nano Lett.*, 2008, **8**, 902–907.
4 A. Peigney, C. Laurent, E. Flahaut, R. Bacsa and A. Rousset, *Carbon*, 2001, **39**, 507–514.
5 M. D. Stoller, S. Park, Z. Yanwu, J. An and R. S. Ruoff, *Nano Lett.*, 2008, **8**, 3498–3502.
6 C. Lee, X. Wei, J. W. Kysar and J. Hone, *Science*, 2008, **321**, 385–388.
7 L. S. Panchakarla, K. S. Subrahmanyam, S. K. Saha, A. Govindaraj, H. R. Krishnamurthy, U. V. Waghmare and C. N. R. Rao, *Adv. Mater.*, 2009, **21**, 4726–4730.
8 Z.-H. Sheng, H.-L. Gao, W.-J. Bao, F.-B. Wang and X.-H. Xia, *J. Mater. Chem.*, 2012, **22**, 390–395.
9 Y. A. Kim, K. Fujisawa, H. Muramatsu, T. Hayashi, M. Endo, T. Fujimori, K. Kaneko, M. Terrones, J. Behrends, A. Eckmann, C. Casiraghi, K. S. Novoselov, R. Saito and M. S. Dresselhaus, *ACS Nano*, 2012, **6**, 6293–6300.
10 D. Wei, Y. Liu, Y. Wang, H. Zhang, L. Huang and G. Yu, *Nano Lett.*, 2009, **9**, 1752–1758.
11 Y. Wang, Y. Shao, D. W. Matson, J. Li and Y. Lin, *ACS Nano*, 2010, **4**, 1790–1798.
12 Z. Jin, J. Yao, C. Kittrell and J. M. Tour, *ACS Nano*, 2011, **5**, 4112–4117.
13 Z. Luo, S. Lim, Z. Tian, J. Shang, L. Lai, B. MacDonald, C. Fu, Z. Shen, T. Yu and J. Lin, *J. Mater. Chem.*, 2011, **21**, 8038–8044.
14 Y. F. Lu, S. T. Lo, J. C. Lin, W. Zhang, J. Y. Lu, F. H. Liu, C. M. Tseng, Y. H. Lee, C. Te Liang and L. J. Li, *ACS Nano*, 2013, **7**, 6522–6532.
15 J. Li, Z. Ren, Y. Zhou, X. Wu, X. Xu, M. Qi, W. Li, J. Bai and L. Wang, *Carbon*, 2013, **62**, 330–336.
16 Z. Wang, P. Li, Y. Chen, J. Liu, H. Tian, J. Zhou, W. Zhang and Y. Li, *J. Mater. Chem. C*, 2014, **2**, 7396–7401.
17 D. Usachov, O. Vilkov, a. Grüneis, D. Haberer, a. Fedorov, V. K. Adamchuk, a. B. Preobrajenski, P. Dudin, a. Barinov, M. Oehzelt, C. Laubschat and D. V. Vyalikh, *Nano Lett.*, 2011, **11**, 5401–5407.
18 A. Lherbier, A. R. Botello-Méndez and J. C. Charlier, *Nano Lett.*, 2013, **13**, 1446–1450.
19 S. H. Park, J. Chae, M.-H. Cho, J. H. Kim, K.-H. Yoo, S. W. Cho, T. G. Kim and J. W. Kim, *J. Mater. Chem. C*, 2014, **2**, 933–939.
20 L. Qu, Y. Liu, J. B. Baek and L. Dai, *ACS Nano*, 2010, **4**, 1321–1326.
21 L. Zhang and Z. Xia, *J. Phys. Chem. C*, 2011, **115**, 11170–11176.
22 A. L. M. Reddy, A. Srivastava, S. R. Gowda, H. Gullapalli, M. Dubey and P. M. Ajayan, *ACS Nano*, 2010, **4**, 6337–6342.
23 Z. S. Wu, W. Ren, L. Xu, F. Li and H. M. Cheng, *ACS Nano*, 2011, **5**, 5463–5471.
24 X. Kong and Q. Chen, *Phys. Chem. Chem. Phys.*, 2013, **15**, 12982–12987.
25 H. M. Jeong, J. W. Lee, W. H. Shin, Y. J. Choi, H. J. Shin, J. K. Kang and J. W. Choi, *Nano Lett.*, 2011, **11**, 2472–2477.
26 H. Wang, T. Maiyalagan and X. Wang, *ACS Catal.*, 2012, **2**, 781–794.
27 T. Matsui, M. Yudasaka, R. Kikuchi, Y. Ohki and S. Yoshimura, *Appl. Phys. Lett.*, 1994, **65**, 2145–2147.
28 Y. Ito, C. Christodoulou, M. V. Nardi, N. Koch, H. Sachdev and K. Müllen, *ACS Nano*, 2014, **8**, 3337–3346.
29 S. Entani, S. Ikeda, M. Kiguchi, K. Saiki, G. Yoshikawa, I. Nakai, H. Kondoh and T. Ohta, *Appl. Phys. Lett.*, 2006, **88**, 153126.
30 M. Yamamoto, S. Obata and K. Saiki, *Surf. Interface Anal.*, 2010, **42**, 1637–1641.
31 G. Imamura and K. Saiki, *J. Phys. Chem. C*, 2011, **115**, 10000–10005.
32 G. Imamura, C. W. Chang, Y. Nabae, M. A. Kakimoto, S. Miyata and K. Saiki, *J. Phys. Chem. C*, 2012, **116**, 16305–16310.
33 G. Imamura and K. Saiki, *J. Phys. Chem. C*, 2014, **118**, 11842–11848.
34 L. Gao, W. Ren, H. Xu, L. Jin, Z. Wang, T. Ma, L.-P. Ma, Z. Zhang, Q. Fu, L.-M. Peng, X. Bao and H.-M. Cheng, *Nat. Commun.*, 2012, **3**, 699.
35 K. Akada, T. Terasawa, G. Imamura, S. Obata and K. Saiki, *Appl. Phys. Lett.*, 2014, **104**, 131602.
36 Z. Fang, V. Chellappan, R. D. Webster, L. Ke, T. Zhang, B. Liu and Y.-H. Lai, *J. Mater. Chem.*, 2012, **22**, 15397–15404.
37 J. E. Field and D. Venkataraman, *Chem. Mater.*, 2002, **14**, 962–964.
38 M. Gao, Y. Pan, L. Huang, H. Hu, L. Z. Zhang, H. M. Guo, S. X. Du and H. J. Gao, *Appl. Phys. Lett.*, 2011, **98**, 033101.
39 A. C. Ferrari and D. M. Basko, *Nat. Nanotechnol.*, 2013, **8**, 235–246.
40 G. W. Cushing, V. Johánek, J. K. Navin and I. Harrison, *J. Phys. Chem. C*, 2015, **119**, 4759–4768.
41 B. Vermang, M. Juel and S. Raaen, *J. Vac. Sci. Technol., A*, 2007, **25**, 1512–1518.
42 G. Franc and A. Gourdon, *Phys. Chem. Chem. Phys.*, 2011, **13**, 14283–14292.
43 J. Cai, P. Ruffieux, R. Jaafar, M. Bieri, T. Braun, S. Blankenburg, M. Muoth, A. P. Seitsonen, M. Saleh, X. Feng, K. Müllen and R. Fasel, *Nature*, 2010, **466**, 470–473.
44 A. L. Pinardi, G. Otero-Irurueta, I. Palacio, J. I. Martinez, C. Sanchez-Sanchez, M. Tello, C. Rogero, A. Cossaro, A. Preobrajenski, B. Gómez-Lor, A. Jancarik, I. G. Stará, I. Starý, M. F. Lopez, J. Méndez and J. A. Martin-Gago, *ACS Nano*, 2013, **7**, 3676–3684.
45 A. L. Pinardi, J. I. Martínez, A. Jančařík, I. G. Stará, I. Starý, M. F. López, J. Méndez and J. Á. Martín-Gago, *Chem. Commun.*, 2014, **50**, 1555–1557.
46 M. Treier, C. A. Pignedoli, T. Laino, R. Rieger, K. Müllen, D. Passerone and R. Fasel, *Nat. Chem.*, 2011, **3**, 61–67.
47 A. Eckmann, A. Felten, A. Mishchenko, L. Britnell, R. Krupke, K. S. Novoselov and C. Casiraghi, *Nano Lett.*, 2012, **12**, 3925–3930.
48 L. G. Cançado, A. Jorio, E. H. M. Ferreira, F. Stavale, C. A. Achete, R. B. Capaz, M. V. O. Moutinho, A. Lombardo,

T. S. Kulmala and A. C. Ferrari, *Nano Lett.*, 2011, **11**, 3190–3196.

49 S. Bhaviripudi, X. Jia, M. S. Dresselhaus and J. Kong, *Nano Lett.*, 2010, **10**, 4128–4133.

50 X. Li, C. W. Magnuson, A. Venugopal, J. An, J. W. Suk, B. Han, M. Borysiak, W. Cai, A. Velamakanni, Y. Zhu, L. Fu, E. M. Vogel, E. Voelkl, L. Colombo and R. S. Ruoff, *Nano Lett.*, 2010, **10**, 4328–4334.

51 N. Bonalumi, T. Bürgi and A. Baiker, *J. Am. Chem. Soc.*, 2003, **125**, 13342–13343.

52 Y. T. Kim, J. a. Dumesic and G. W. Huber, *J. Catal.*, 2013, **304**, 72–85.

53 T. T. Pham, L. L. Lobban, D. E. Resasco and R. G. Mallinson, *J. Catal.*, 2009, **266**, 9–14.

54 J. R. Roy, M. a. Laliberté, S. Lavoie, M. Castonguay and P. H. McBreen, *Surf. Sci.*, 2005, **578**, 43–56.